Arthropod Structure & Development 46 (2017) 552–563

Contents lists available at ScienceDirect

Arthropod Structure & Development

journal homepage: www.elsevier.com/locate/asd

The sensory arrays of the ant, *Temnothorax rugatulus*

Fiorella Ramirez-Esquivel [a, *], Nicole E. Leitner [b], Jochen Zeil [a], Ajay Narendra [c]

[a] Research School of Biology, The Australian National University, Canberra, ACT 2601, Australia
[b] Department of Ecology and Evolutionary Biology, University of Arizona, PO Box 210088, Tucson, AZ 85721-0088, USA
[c] Department of Biological Sciences, Macquarie University, Sydney, NSW 2109, Australia

ARTICLE INFO

Article history:
Received 3 January 2017
Accepted 22 March 2017
Available online 12 April 2017

Keywords:
Sensilla
Compound eyes
Intraspecific variation
Small sensory arrays

ABSTRACT

Individual differences in response thresholds to task-related stimuli may be one mechanism driving task allocation among social insect workers. These differences may arise at various stages in the nervous system. We investigate variability in the peripheral nervous system as a simple mechanism that can introduce inter-individual differences in sensory information. In this study we describe size-dependent variation of the compound eyes and the antennae in the ant *Temnothorax rugatulus*. Head width in *T. rugatulus* varies between 0.4 and 0.7 mm (2.6–3.8 mm body length). But despite this limited range of worker sizes we find sensory array variability. We find that the number of ommatidia and of some, but not all, antennal sensilla types vary with head width.

The antennal array of *T. rugatulus* displays the full complement of sensillum types observed in other species of ants, although at much lower quantities than other, larger, studied species. In addition, we describe what we believe to be a new type of sensillum in hymenoptera that occurs on the antennae and on all body segments. *T. rugatulus* has apposition compound eyes with 45–76 facets per eye, depending on head width, with average lens diameters of 16.5 μm, rhabdom diameters of 5.7 μm and inter-ommatidial angles of 16.8°. The optical system of *T. rugatulus* ommatidia is severely under focussed, but the absolute sensitivity of the eyes is unusually high.

We discuss the functional significance of these findings and the extent to which the variability of sensory arrays may correlate with task allocation.

1. Introduction

Ants are social insects and as such their societies are characterised by the division of labour among individuals. This includes the distribution of different tasks among workers. Task allocation among workers is based on genetic and epigenetic variation, differences in developmental conditions and trajectories, and experience-dependent processes, including learning and memory (e.g. Charbonneau and Dornhaus, 2015a; Maleszka, 2016). One potential mechanism involved in task allocation lies in the variable thresholds with which individuals respond to task-related cues, whether they be sensory or cognitive (e.g. Charbonneau and Dornhaus, 2015a). This may apply even in cases where there is limited variability among individuals, such as in monomorphic species. Variations in response thresholds can be due to any number of reasons, amongst them genetic and epigenetic variation, developmental conditions, differences in body size or age (reviewed in Charbonneau and Dornhaus, 2015a). Independent of underlying causes, one relatively easily quantifiable trait that must affect response thresholds is the number and type of sensors available to an ant. Investigating the variation in this trait with the aim of correlating it with variations in task allocation for any given species of ant may establish an important link between genetic, epigenetic and developmental processes and the behavioural plasticity underlying task allocation in social insects.

Body size variation is associated with differences in the compound eyes and the antennal array of sensilla, which can lead to functional differences among workers. The eyes and antennae are the two most important sensory organs for providing ants with information about the external environment. Combined, these sensory organs detect visual, chemical and mechanical cues as well as information about temperature, humidity and CO_2 levels. In bumblebees, differences in the number of antennal sensilla and

* Corresponding author.
E-mail addresses: fiorella.ramirez-esquivel@anu.edu.au (F. Ramirez-Esquivel), nefischer@email.arizona.edu (N.E. Leitner), jochen.zeil@anu.edu.au (J. Zeil), ajay.narendra@mq.edu.au (A. Narendra).

http://dx.doi.org/10.1016/j.asd.2017.03.005
1467-8039/

ommatidia have been shown to respectively affect a worker's odour sensitivity and visual resolution (e.g. Spaethe and Chittka, 2003; Spaethe et al., 2007). At the behavioural level, larger bumblebee workers are more likely to engage in foraging behaviours than their smaller counterparts (Spaethe and Chittka, 2003; Spaethe et al., 2007). Although having a larger body-size may be advantageous for a number of reasons it is likely that increased sensory capabilities contribute towards larger workers being more efficient foragers.

Here, we examine both the compound eyes and the antennae of *Temnothorax rugatulus* ants, the behaviour of which has been well documented, to identify morphological variations potentially affecting individual behaviour. We investigate whether there are body-size dependent differences in the sensory arrays of workers.

2. Methods

2.1. Study site and study species

Worker ants for this study were opportunistically sampled from a single experimental colony. All ants were collected indiscriminately and preserved in ethanol. The colony was collected from the Santa Catalina mountain range, Tucson, Arizona, USA (32°23′43.00″N, 110°41′27.69″W) in May 2015. In the laboratory, the colony was housed in an artificial nest and periodically fed with sugar solution and dead fruit flies (for full methods see: Charbonneau and Dornhaus, 2015b). All imaging of the eyes and antennae was done using this single colony.

Body size and head width variation among workers was recorded by photographing dead specimens under dissecting microscopes (Olympus SZX9, Nikon DS-Fi1). Measurements of the head width (measured in dorsal view just behind the compound eyes) were taken in a total of 100 workers; the sample was made up of 46 workers from the colony mentioned above plus 54 workers from another laboratory colony collected at the same location to boost sample size (the mean and standard deviation were identical for both colonies). Additionally, body length (clypeus to the end of the gaster) and head length (clypeus to apex) measurements were taken for comparison. Measurements were taken from digital images using ImageJ 1.45s (Rusband, National Institutes of Health, USA).

2.2. SEM specimen preparation

Whole specimens were stored in 70% ethanol. The amputated antennae or whole heads were then mounted on aluminium stubs using conductive carbon tape. Specimens were coated with Au/Pd (60:40) for 2 min at 20 mA and imaged on a Hitachi S-4300 SE/N scanning electron microscope. For detailed methods see Ramirez-Esquivel et al. (2014).

2.3. Compound eye histology

For the study of the internal anatomy of the eyes live specimens were immobilised using wax under a dissection microscope, the mandibles were removed and the back of the head capsule was quickly opened up. The remainder of the head capsule, bearing the two compound eyes, was immediately placed in ice-cold aldehyde fixative (50:50 mixture of 4% formaldehyde and 4% glutaraldehyde, pH 7.2) and left for 5 h while the remainder of the body was immersed in 100% ethanol to kill the ant. The samples were then rinsed in PBS (5 × 3 minutes) and post-fixed in 2% OsO_4 solution for 90–120 min. The samples were once again rinsed in PBS (5 × 3 minutes) and stained with 2% uranyl acetate overnight. After rinsing, as above, the samples were dehydrated in an ethanol series (50–100%) and transferred into propylene oxide for resin infiltration. The Epoxy (Epon) infiltrated tissues were polymerised in an oven at 60° for 12 h. For detailed methods see Greiner et al. (2007) and Narendra et al. (2013).

Samples were sectioned with a HistoJumbo diamond knife (Diatome, Biel/Bienne, Switzerland) to 2 μm thickness on a Leica EM UC7 ultramicrotome, mounted on glass slides, heat fixed and stained for contrast with toluidine blue. They were later imaged on a Zeiss Axioskop compound microscope equipped with a SPOT Flex 16 MP colour camera.

2.4. Image processing and measurements

All image processing, including SEM colourisation, was carried out with CorelDraw® Graphics Suite X6 (2012 Corel). Measurements were made directly from digital images with ImageJ 1.45s (Rusband, National Institutes of Health, USA).

To estimate the variability of the antennal sensillum array between different individuals we quantified the abundance of the different types of sensilla and measured the length of sensilla basiconica, trichodea and trichodea curvata in six worker ants of different sizes (head width varied from 0.46 to 0.63 mm). We focused on the dorsal surface of the antenna but also examined the ventral surface in three individuals for comparison. Antenna area estimations are based on measurements of the visible area from SEM images, not taking into account the effects of curvature. Sensillum length was measured on sensilla which were clearly visible in profile (for full details see Ramirez-Esquivel et al., 2014). We concentrated on the filiform chemoreceptors as these were relatively plentiful (unlike peg-in-pit sensilla, i.e. sensilla coeloconica, ampullacea, coelocapitular and campaniformia).

Compound eye facets were counted in SEM images. Internal eye structures were measured in semi-thin sections from three individuals. These measurements were used to calculate resolution (inter-ommatidial and acceptance angles) and optical sensitivity (the eye's ability to capture photons when viewing a scene of broad spectral content) (Land and Nilsson, 2012). Optical sensitivity, S, is given in μm^2 sr (Land, 1981; Warrant and Nilsson, 1998) as:

$$S = \left(\frac{\pi}{4}\right)^2 A^2 \left(\frac{d}{f}\right)^2 \left(\frac{kl}{2.3 + kl}\right),$$

where, A = facet diameter (μm); d = diameter of the rhabdom (μm); f = focal length, determined by the distance from the nodal point of the lens to the tip of the rhabdom (μm); l = the rhabdom length (μm); k = absorption coefficient, assumed to be 0.0067 μm^{-1} (see Warrant and Nilsson, 1998). We used the thick lens equation (see Stavenga, 2003; Schwarz et al., 2011) to determine the position of the nodal point, the focal length and the location of the focal plane, assuming a homogeneous refractive index of the lens and the crystalline cone.

3. Results

3.1. Gross morphology and body size

T. rugatulus are yellowish brown ants, with rugose sculpturing on the cuticle of the head, thorax and petiole (Fig. 1A, B). Workers were small with a body length of 2.6–3.8 mm (n = 46). Throughout this study we have chosen to omit body length from the analyses and use head width as a proxy for body size, since body length, which includes the gaster, can vary greatly according to nutritional state and satiety. Head width is a commonly used proxy in the ant literature (e.g. Hölldobler and Wilson, 1990; Kaspari and Weiser,

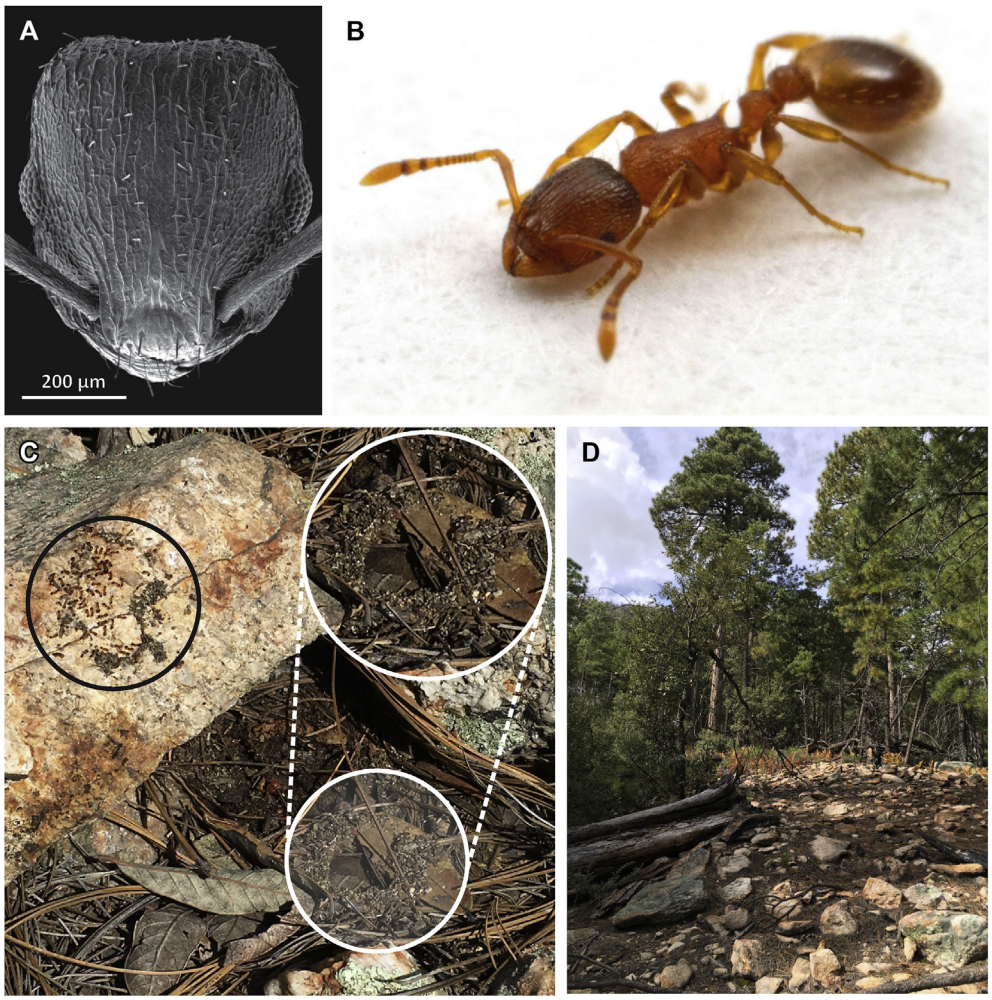

Fig. 1. Overview of the study species *Temnothorax rugatulus*. (A) Scanning electron micrograph of the worker head showing laterally placed compound eyes and characteristic rugosities of the head cuticle. (B) Overview photograph of worker: note yellow-brown colouration and club antennae. Photo credit: Michele Lanan (C) Nesting site under an upturned rock: the white circle indicates the nest location on the substrate; the black circle indicates the corresponding surface on the upturned rock with workers and queen clinging on. (D) Overview of the environment surrounding the nest site, the rocky landscape is dominated by pine trees with patchy understorey.

1999; Tschinkel et al., 2003), and has been previously used to describe size variation in *T. rugatulus* (Westling et al., 2014), where it scales linearly with both body length ($R^2 = 0.67$, $n = 46$) and head length ($R^2 = 0.93$, $n = 54$). We found head width varied from 0.45 to 0.66 mm ($n = 100$), representing a variation of approximately ±20% around the mean (Fig. 2). The size distribution was similar to a previously described distribution (Westling et al., 2014) but with a relatively limited range of head widths (Fig. 2). It did not significantly deviate from a normal distribution (D'Agostino and Pearson test, $P = 0.7127$).

3.2. Antennal array

3.2.1. General anatomy and characteristics of the antenna

The antennae consisted of a scape, a pedicel and nine flagellar segments. The pedicel and the flagellum are jointly referred to as the funiculus (Fig. 3A). Of the funicular segments, F1-3 were the largest and formed a club while F4-9 were greatly reduced and formed a thin straight shaft (Fig. 3A). The dorsal surface area of the club was in fact over three times larger than that of the shaft (Fig. 3B), despite being comprised of fewer segments. Smaller funicular segments bore fewer sensilla, and chemosensitive sensilla in particular dropped in abundance as segments became smaller and were altogether missing from the small shaft segments (Fig. 3C). Larger workers tended to have a larger total antennal area ($R^2 = 0.70$, $n = 6$ workers), where an increase of 0.01 mm in head width was accompanied by an increase of approximately 900 μm^2 of antennal area.

3.2.2. Sensillum types and their distributions

We surveyed the dorsal surface of the entire antenna and found ten different types of sensilla, each with their own particular distributions, which were consistent across individuals (Fig. 4A). Seven of the ten types of sensilla were confined to the club: sensilla basiconica, trichodea, trichodea curvata, trichoid-II, coeloconica, ampullacea and coelocapitular (Fig. 4A–C). The filiform mechanoreceptors, sensilla chaetica, were present throughout the antenna (Fig. 4A, B) while sensillum campaniformium (Fig. 4D) was restricted to the distal border of the pedicel (Fig. 4A).

We discovered a pair of peculiar branched sensilla on the scape, which to the best of our knowledge have not been previously described in hymenoptera. This sensillum has a hand-like appearance with variable numbers (3–10) of digitate or finger-like projections (Fig. 5A, C). These sensilla project over the scape-pedicel

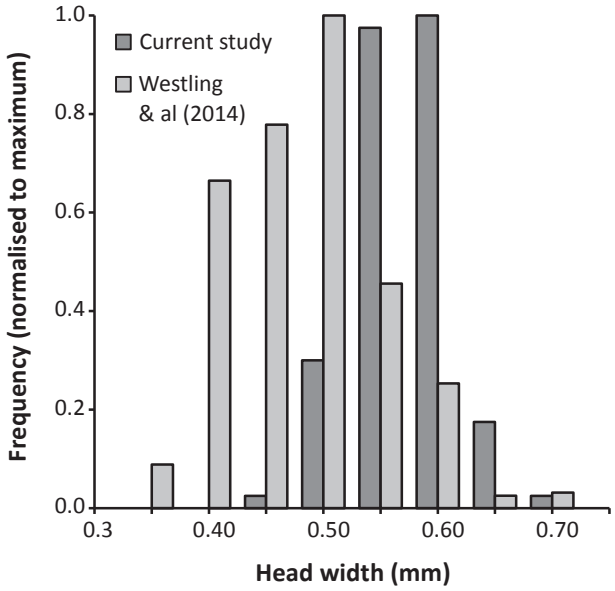

Fig. 2. Frequency histogram of worker size variation in *Temnothorax rugatulus*. Head width acts as a proxy for body size. Data from the current study overlayed with previous data from Westling et al. (2014) for comparison (n = 100 and 522 respectively). See Discussion for details.

joint and generally occurred as a single pair on the dorsal surface (Fig. 5A, C), although there can occasionally be 1 or 3 sensilla instead of 2. The peg length was longer than in most other sensilla (see "Size of sensilla" section below), at 39.0 ± 5.5 μm (mean ± s.d., n = 11). Similarly branched sensilla are present on the dorsal surface of the head, mesosoma and gaster (Fig. 5B, E, F) where they are longer (head: 53.0 ± 8.1 μm, n = 11; mesosoma: 62.8 ± 10.2 μm, n = 15; gaster: 68.5 ± 8.6 μm, n = 16) and have their projections arranged in different configurations (Fig. 5C, D, G, H). It is possible that not all of these sensilla are homologous.

3.2.3. Sensillum variation among individuals: size and numbers of sensilla

In order to gather sufficient, reliable data to investigate the effects of worker size variation on the sensillar array we concentrated on the filiform sensilla (sensilla basiconica, trichodea, trichodea curvata, chaetica and TII) on the dorsal surface of the club (Fig. 4B), as these were most abundant.

3.2.3.1. Numbers of sensilla. The number of sensilla varied with worker size but the manner in which they varied was dependent on the sensillum type. The relative numbers of sensilla basiconica and Trichoid II (TII) increased considerably and consistently with head width (from 8 to 13 and from 20 to 36 respectively), and in both of these cases there was a strong, positive, linear relationship between the number of sensilla and worker head width normalized to maximum ($R^2 = 0.98$ and 0.81 respectively, $F < 0.05$, orange and red dashed lines, Fig. 6A). The head width of workers examined varied from 0.46 to 0.63 mm which equates to a 36% increase in head width (relative to the minimum), compared to a 63% increase in sensilla basiconica and an 80% increase in TII sensilla. In contrast, there was no strong correlation ($R^2 < 0.30$, $F > 0.05$) between numbers of sensilla and worker size in the case of sensilla trichodea, trichodea curvata and chaetica (green and dark purple dashed lines, Fig. 6A).

The average absolute abundance of different sensillum types differed greatly and as a consequence so did their relative

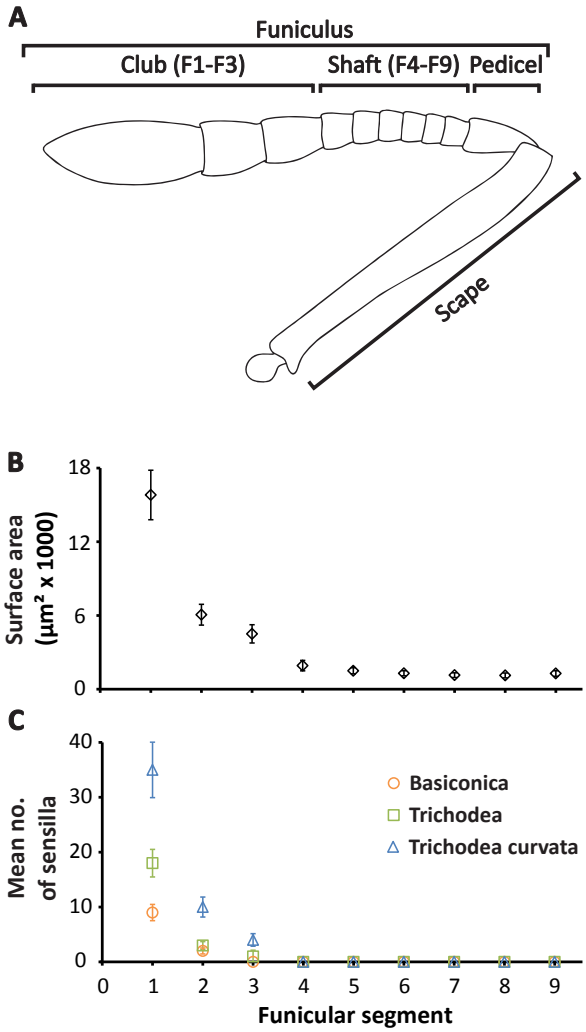

Fig. 3. Overview of the antennal anatomy of *Temnothorax rugatulus*. (A) Parts of the antenna including the club (segments F1 to F3), shaft (F4 to F9), pedicel and scape. (B) Size variation across funicular segments. (C) Average number of filiform chemosensitive sensilla across funicular segments. Error bars represent standard deviations, n = 5.

contributions to the total sensillum array (Fig. 6B). The vast majority (72%) of the sensilla found on the club were mechanoreceptive sensilla chaetica while the remaining 28% of filiform sensilla were comprised of four different types of chemoreceptors and a putative chemoreceptor. Among the chemoreceptors the smallest contribution (3%) was made by sensilla basiconica and the largest by sensilla trichodea curvata (12%) (Fig. 6B).

The relative increase from the minimum to the maximum observed abundance of a sensillum type across different individuals was unrelated to the absolute abundance of that sensillum (Fig. 6C). That is to say, the relative variability of a sensillum type was unrelated to its absolute abundance. The most variable sensilla were sensilla basiconica (63% increase relative to the minimum) and TII (80%) while the least variable were sensilla chaetica (38%) and trichodea (19%).

Comparing the dorsal (n = 5 workers) and ventral (n = 3 workers) surfaces of the club, we found that the ventral surface has, overall, fewer sensilla. As compared to the dorsal surface, there were approximately 20% fewer sensilla trichodea and trichodea curvata and approximately 70% fewer TII sensilla on the ventral surface. Sensilla chaetica did not vary dramatically between the two surfaces while sensilla basiconica were similar in abundance

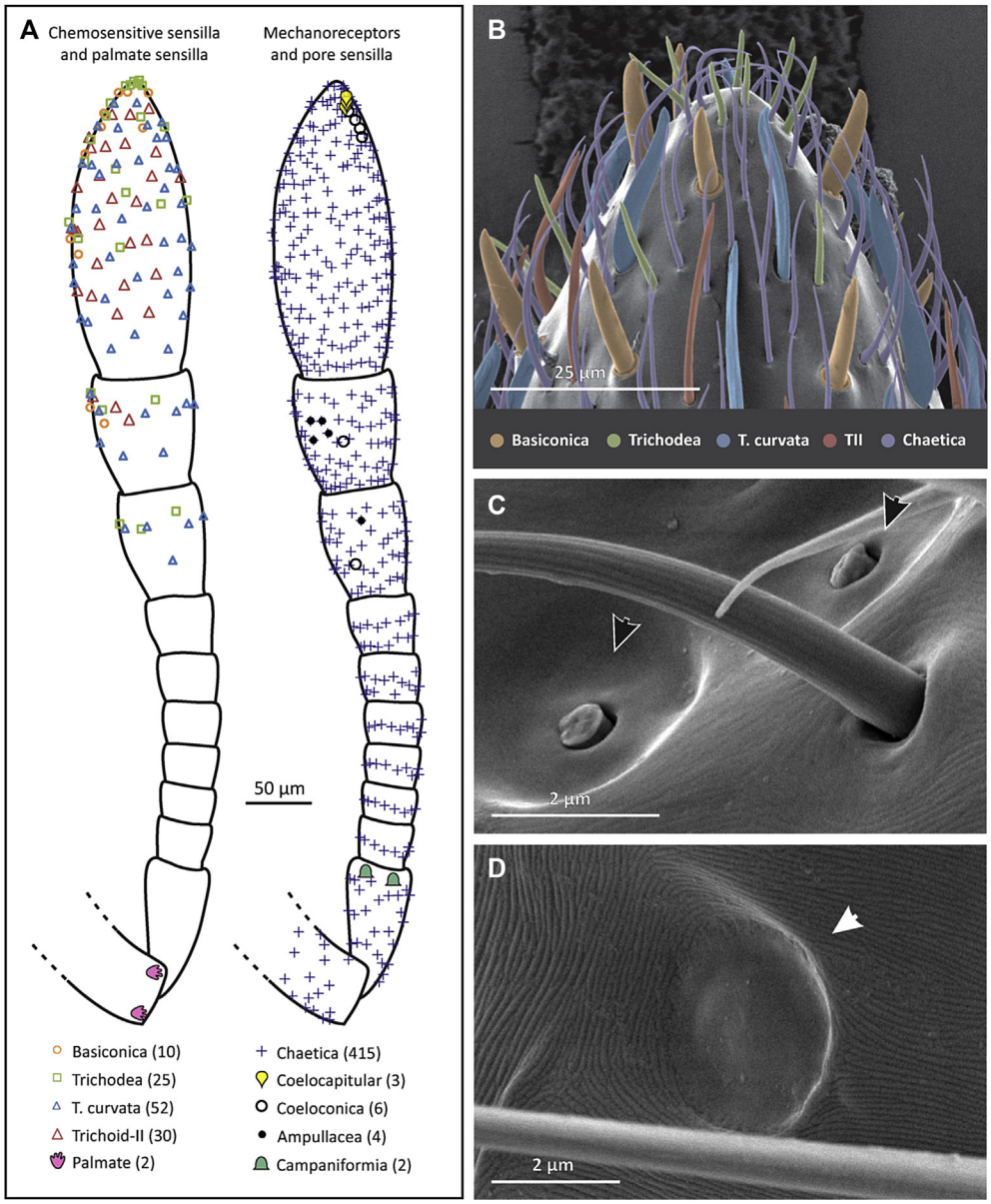

Fig. 4. Types of sensilla and their distributions on the *Temnothorax rugatulus* antenna. (A) Example map of locations of filiform chemosensilla and palmate sensilla (left), and sensilla chaetica and peg-in-pit sensilla (right) on the dorsal surface of the antenna of *Temnothorax rugatulus*. Data are from the right antenna of a single worker (head width = 0.58) but mapped separately for clarity. Legend lists sensillum types and abundances. (B) Colourised SEM of the antennal tip; colour-coded are the various types of filiform sensilla. Two examples of peg-in-pit sensilla: (C) a pair of coelocapitular sensilla (black arrows) and (D) sensilla campaniformia (white arrow).

both dorsally and ventrally or, in the case of one worker, they were more abundant ventrally.

3.2.3.2. Size of sensilla. Here we restricted our analysis to the three filiform chemosensilla: sensilla basiconica, trichodea and trichodea curvata (see methods). Sensilla basiconica and trichodea were of similar length while sensilla trichodea curvata were much longer (Fig. 7A). We found that sensillum size could not be predicted by worker head width. Sensilla basiconica ranged continuously from 10 to 20 µm (n = 38 sensilla, 6 workers) with approximately the whole range of variation being displayed in every individual examined independently of head width (data not shown). Similarly sensilla trichodea ranged from 8 to 18 µm (n = 38 sensilla, 6 workers) and trichodea curvata from 20 to 34 µm (n = 69 sensilla, 6 workers). Within individuals, sensilla are roughly organised from smallest to largest on the apical segment. Peg length varied with proximity to the apex of the antenna following a power relationship where the closer a sensillum was to the tip the shorter its peg (Fig. 7B).

3.3. Optical system

T. rugatulus workers possess a pair of apposition compound eyes and no ocelli. The compound eyes were laterally placed (e.g. Fig. 1A) and measured 107.0 ± 10.2 µm (mean ± s.d.) along the dorso–ventral axis (n = 17) and 141.0 ± 15.8 µm along the anterior–posterior axis (n = 17). Eye size was not correlated with head width ($R^2 < 0.05$). Each eye was made up of 55.2 ± 6.5 ommatidia (mean ± s.d., n = 39, Fig. 8A); however, the number of ommatidia varied considerably with worker size, ranging from 45 to 76

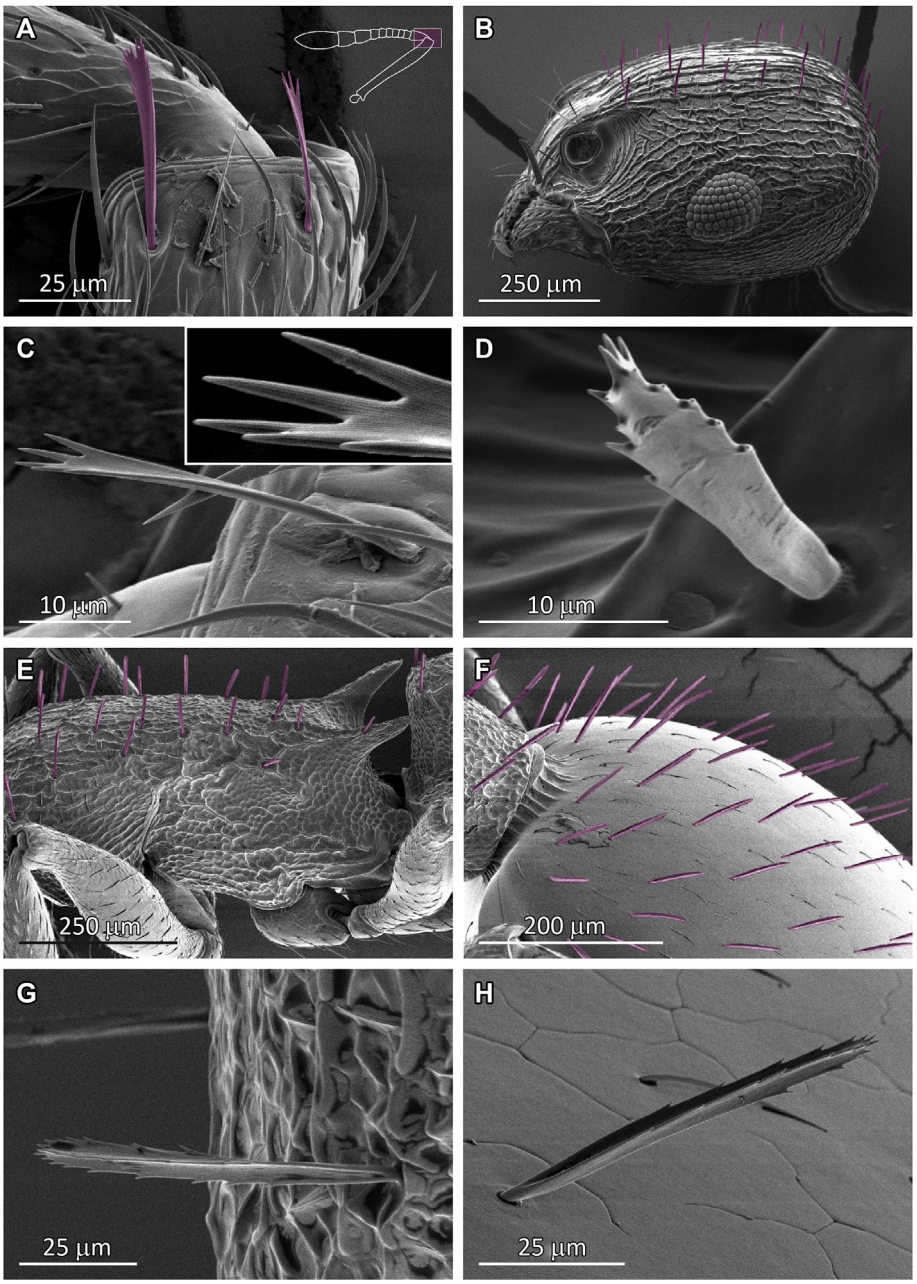

Fig. 5. Previously undescribed, branched 'palmate' sensilla as seen in various body parts of *Temnothorax rugatulus*. 'Palmate' sensilla at the (A, C) scape-pedicel joint, (B, D) dorsal surface of the head, (E, G) dorsal surface of the mesosoma and (F, H) dorsal surface of the gaster. The 'palmate' sensilla are artificially colourised in pink in panels A, B, E and F.

(Fig. 8B). This represents, relative to the mean, a 19% decrease in the ants with the fewest facets and a 37% increase in the ants with the most. Within individuals, the number of facets between the left eye (55.25 ± 1.94; mean ± s.d.) and the right eye (55.94 ± 2.01) did not differ significantly (paired t-test, n = 16, p = 0.102, t = 1.741, df = 15). The facets were not arrayed to form a regular hexagonal pattern as in larger ants (e.g. Narendra et al., 2011) but were irregularly arranged (Fig. 8A) (see also Pix et al., 2000).

Across the horizontal plane the visual field spanned approximately 120°, and the maximum number of facets in a horizontal row ranged between individuals from 8 to 11 facets, as judged from horizontal sections (Fig. 8C). This translates into horizontal inter-ommatidial angles ($\Delta\phi$) of between 11° and 15°. In the vertical plane the field of view spans about 130° with a maximum of 7–9 facets ($\Delta\phi = 14°–19°$). The full extent of the visual field of one eye is thus approximately 15,600 deg^2 (120°x130°) with each ommatidium covering 15,600/55 = 284 deg^2, which equates to an average inter-ommatidial angle of 16.8°. The average facet diameter is 16.5 ± 1.1 μm (range: 14.7–19.0 μm; n = 41), which produces a blur circle half-width of $\Delta\rho_{lens}$ = 1.5–1.9 μm ($\Delta\rho_{lens} = \lambda/A$ [rad], with wavelength of light λ = 0.5 μm; facet diameter A = 16.5 μm). Measuring the facet diameters of the whole central horizontal row in 22 workers revealed that facet diameter was not correlated with head width ($R^2 < 0.13$). The photosensitive structures (the rhabdoms) are 5.7 ± 0.0 μm wide (n = 3; Fig. 8E) and approximately 27.4 ± 1.9 μm long (n = 6; Fig. 8C).

Given they had unusually large rhabdoms for a day-active species, we aimed to determine their optical sensitivity. For this, we first determined the distance between the nodal point of the lens and the focal plane by applying the thick lens equation with the

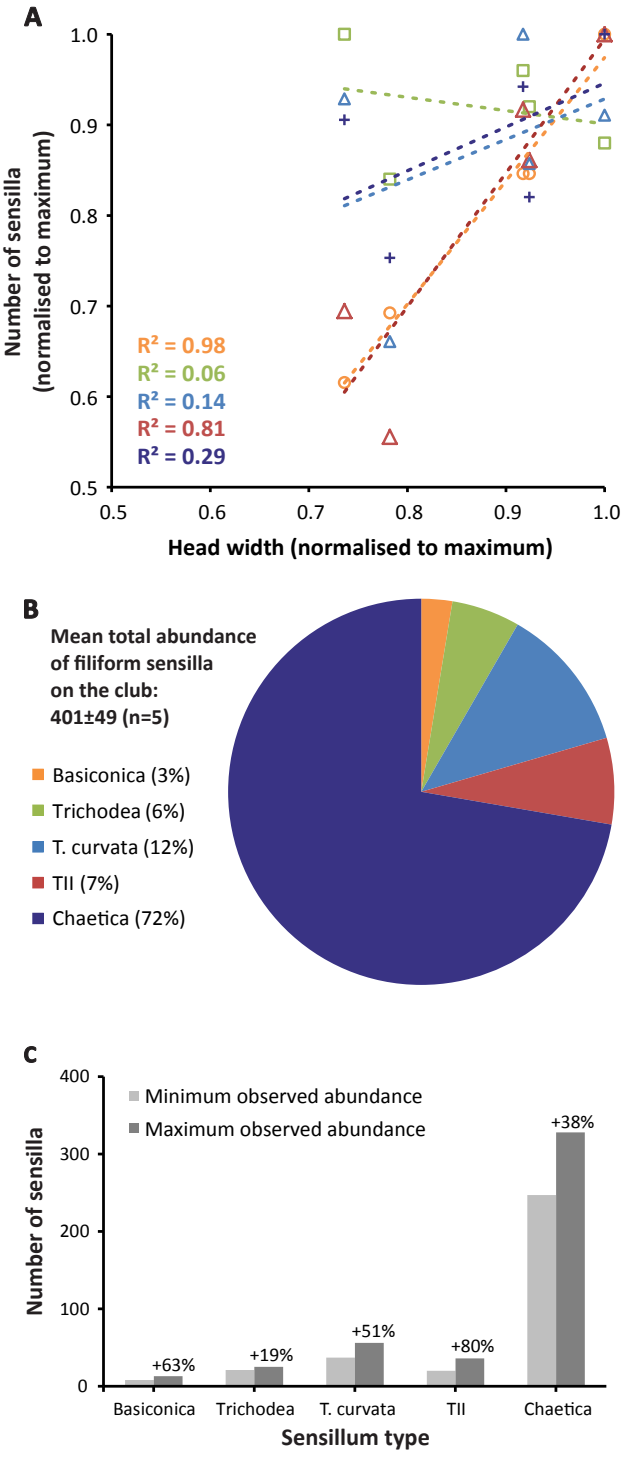

Fig. 6. Abundance of filiform sensilla on the club of *Temnothorax rugatulus*. (A) Variation in sensillum abundance on the club among workers of different size (n = 5 workers). Sensillum types colour-coded as per panel B. Note that head width normalised to maximum is plotted on the x-axis. (B) Average contributions of different filiform sensillum types towards total average filiform sensilla on the club. (C) Comparison of maximum and minimum observed abundances for each sensillum type, the percentage increase from minimum to maximum (relative to the minimum value) is stated for each sensillum type.

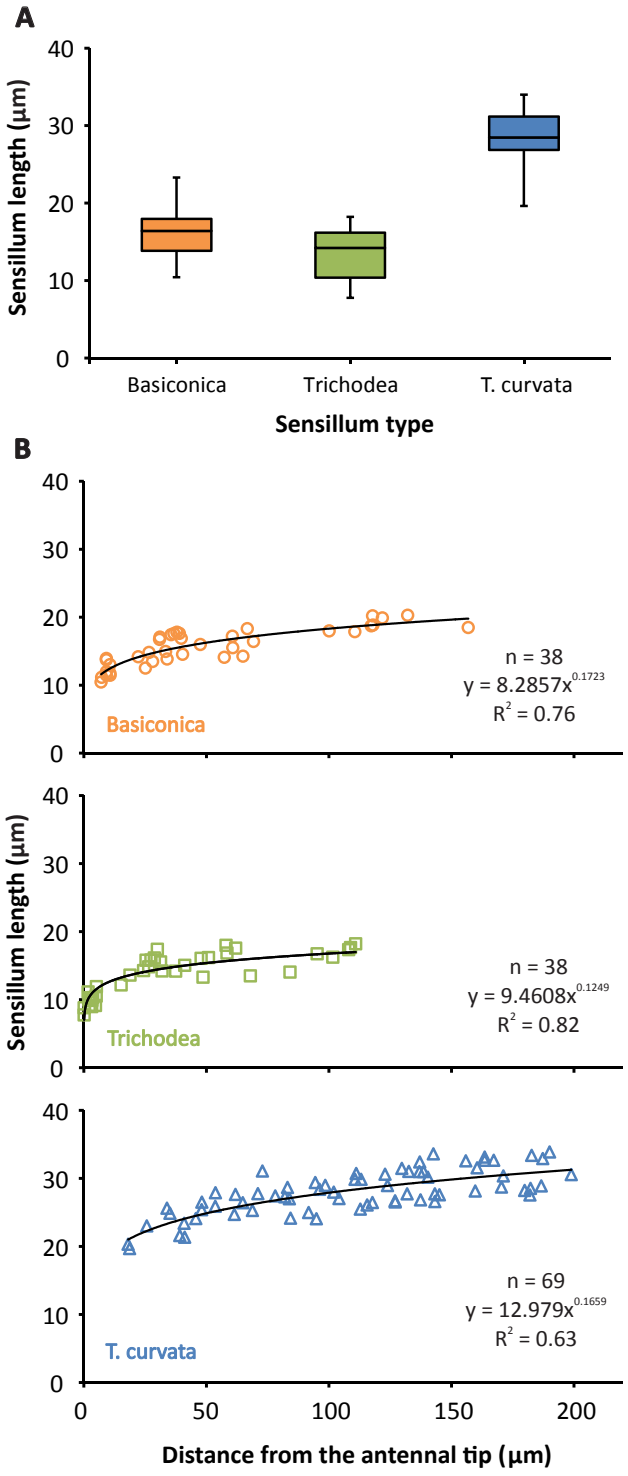

Fig. 7. Variability in peg length of filiform chemoreceptors in *Temnothorax rugatulus*. (A) Comparison of the distribution of peg lengths in sensilla basiconica, trichodea and trichodea curvata. Boxplot represent median, 1st and 3rd quartile, and minimum and maximum peg length. (B) Peg lengths relative to distance from the tip of the antenna for three sensilla. Sensilla closer to the tip tend to be shorter.

outer lens surface radius of r1 = 11.2 µm (n = 3), the inner lens radius r2 = −6.1 µm (n = 3), the distance between vertices 11.1 µm (n = 3) and refractive indices of 1.43 for the lens and 1.34 for the crystalline cone, assuming a uniform distribution of refractive indices in both compartments. Interestingly, these parameters place the plane of best focus more than 10 µm proximal of the distal tip of the rhabdom (Fig. 8D, red cross). Taking the distance between the distal tip of the rhabdom and the nodal point (9.0 µm, see Fig. 8D) as the effective focal distance for the acceptance angle of the rhabdom, we arrive at an acceptance angle $\Delta\rho_{rhabdom} = 36^{\circ}$

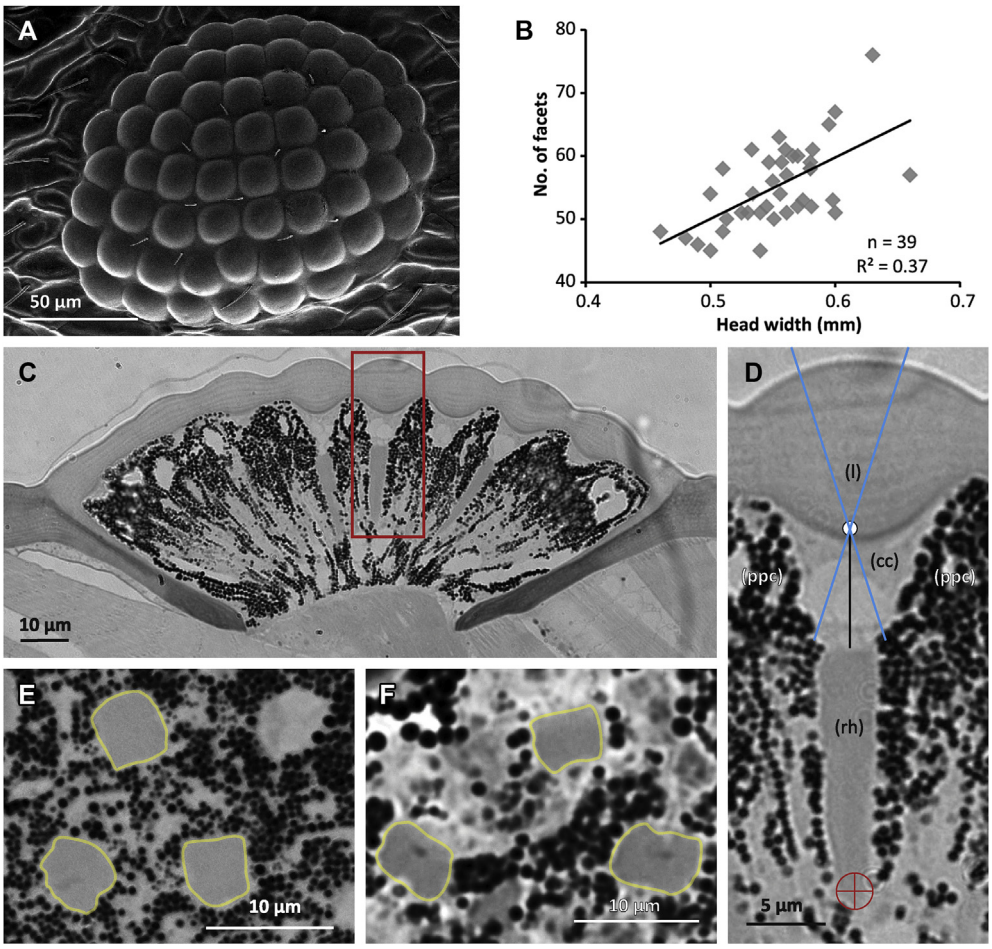

Fig. 8. Eye anatomy of *Temnothorax rugatulus* worker. (A) Overview Scanning Electron Micrograph of the compound eye. (B) Relation between the number of facets and head width. (C) Horizontal section through the compound eye showing longitudinal sections of the ommatidia at the equator of the eye. Red rectangle marks area shown enlarged in panel D. (D) A single ommatidium with its lens (l), crystalline cone (cc), rhabdom (rh) and primary pigment cells (ppc). White circle marks nodal point, black line focal length, and blue lines the approximate limits of angular sensitivity. Red cross marks the calculated plane of best focus, see text for detailed explanation. (E) Cross-section at the level of distal rhabdoms in the frontal region of the eye. (F) Cross-section of the distal rhabdoms of the dorsal rim area of the eye. Outline of the rhabdoms is shown in yellow.

($\Delta\rho_{rhabdom} = d/f$ [rad], with rhabdom diameter d and focal length f), which is only slightly larger than the optimal value of twice the average inter-ommatidial angle of 16.8°. It needs to be noted, however, that the light distribution at this point in the optical pathway is much more diffuse compared to the focal plane. With this value of the acceptance function ($\Delta\rho_{rhabdom}$) the optical sensitivity of the *T. rugatulus* eye would be comparatively high for a miniature compound eye at 4.1 μm^2 sr^{-1} (c.f. Fischer et al., 2011; Makarova et al., 2015), even compared with large night-active bull ants (1–1.6 μm^2 sr^{-1}; (Greiner et al., 2007)) and night-active bees and wasps (2.7 μm^2 sr^{-1}, (Warrant and Dacke, 2011)).

Another feature of interest in the *T. rugatulus* eye was that while most rhabdoms have circular or almost square cross sections (Fig. 8E), a few rhabdoms in the dorsal region of the eye are rectangular in shape, with the long axis measuring 4.4 ± 0.4 µm (n = 4), on average 1.44 times wider than the short axis (Fig. 8F). Such modified rhabdoms are typical for the dorsal rim area (DRA) of insect compound eyes, which is involved in the detection of polarized sky light.

4. Discussion

Despite being a popular study system for behavioural studies there have been no descriptions of the sensory systems of *Temnothorax* ants. We present detailed descriptions of the compound eyes and the antennal sensilla array uncovering some unexpected features. We compare variability between workers and speculate on the possible functional implications of such variation.

The workers of *T. rugatulus* we examine vary in body-size by ±20% around the mean. Accompanying this variation there are quantifiable differences in the elaboration of the sensory arrays. Larger workers tend to have larger antennae with more sensilla basiconica and TII sensilla as well as eyes with more ommatidia. However, body-size alone does not explain all of the variation observed. Most sensillum types did not scale with size and body-size only explained about half of the variation seen in facet numbers ($R^2 = 0.47$, Fig. 8). These trends should result in a certain degree of variation in the sensory information gathering capabilities of individuals in a manner that is linked to, but not exclusively dependent on, body-size. Unfortunately, the opportunistic nature of our sample prevented us from behaviourally identifying intranidal and extranidal workers and the limited sample size meant we did not capture the full range of body-size variation previously described (Westling et al., 2014). Notwithstanding these limitations, we believe that the degree of variability we observed warrants further studies incorporating behavioural observations.

4.1. The antennal array

Temnothorax ants rely on pheromones to orchestrate complex behaviours such as colony emigrations and communication among

nest-mates. During recruitment to new nest sites, for example, workers leading tandem runs discharge a recruitment pheromone from the poison gland (Möglich et al., 1974). Nest scouts use pheromone markings to select favourable nests during colony emigrations (Cao and Dornhaus, 2012) and secrete negative signals to prevent fellow scouts from selecting unsuitable nest sites (Franks et al., 2007; Stroeymeyt et al., 2011, 2014; Sasaki et al., 2014). Finally and perhaps most remarkable of all, some *Temnothorax* species lay not only colony-specific but also individually distinct trails. Experiments have shown that individuals are able to identify and preferentially follow their own trails (Maschwitz et al., 1986). It is clear then that *Temnothorax* ants are capable of behaviours which rely on sophisticated chemosensory abilities. Perhaps then it comes as no surprise that despite their small size *T. rugatulus* display the full complement of sensillum types observed in larger ant species, although at much lower numbers (see Table 3 in: Ramirez-Esquivel et al., 2014). The low numbers of sensilla may mean that small variations in the sensillum array may have a significant impact on the sensory capabilities of individuals, which may result in behavioural differences. To study the variability of the antennal array we compared sensillum sizes and numbers across individuals of different sizes.

It is hard to assess the functional significance of variations in sensillum size. Steinbrecht (1973) found in *Bombyx mori* that long sensilla trichodea almost always were innervated by two receptor cells, while a shorter type of sensilla trichodea contained one to three receptor cells. The situation was different for sensilla basiconica, with large sensilla containing three and a smaller form of the sensillum containing only one receptor cell. In addition, at least in flies, dendritic branching patterns can be quite complicated independently of sensillum size (Lewis, 1971). So all we can say at the moment is that larger sensilla may contain more wall pores and longer dendrites and thus could express more receptor proteins, which would make them more sensitive. However, sensillum length measurements from three filiform sensilla showed quite considerable variability within individuals and no clear differences in sensillum size between different individuals. There was no relationship between sensillum length and head width. This result is consistent with previous observations (Ramirez-Esquivel et al., 2014; van der Woude and Smid, 2015). At this point it is not clear why there is such dramatic intra-individual size variation in sensilla, but one possibility is that packing of both external structures, such as the cuticular elements of the sensilla, and internal structures, such as the underlying neurons, may constrain the size of sensilla in certain locations of the antenna (Schneider, 1964).

In contrast, the number of sensilla of a given type varied from one individual to another, but not all sensilla are affected by changes in head width in the same way. While sensilla chaetica and trichodea curvata were present in variable numbers without a clear dependence on head width, sensilla trichodea seemed to remain relatively constant across different head widths. This could point to a very specific and narrow function unrelated to size or task allocation or to a density dependent function. In contrast, sensilla basiconica and TII consistently increased with head width, suggesting that perhaps extranidal workers benefit from enhancing these sensory channels to perform more informationally demanding behaviours such as foraging.

The functional significance of relative increases in sensillum abundance with increasing head width is not immediately obvious and cannot be ascertained with certainty based on external anatomy alone. However, the variability we observe is an encouraging sign that differences in the peripheral component of ant chemosensation may produce individual differences in how chemical cues are perceived and therefore drive task specialisation.

There are many aspects of the chemosensory array that may affect how an ant perceives an odour cue including the specificity and sensitivity of the chemoreceptors present in the olfactory receptor neurons (ORNs) (e.g. Duchamp-Viret et al., 1999; Sachse et al., 1999), the number of ORNs, the combinations of olfactory receptors present in a single sensillum (e.g. Getz and Akers, 1995), and how olfactory information is organised in the antennal lobe and how it outputs into higher order processing centres of the brain (e.g. Faber et al., 1999; Sachse et al., 1999; Galizia and Menzel, 2000). Of all these variables we can only speculate on the number of ORNs based on our data. Although sensillum numbers do not directly measure ORN numbers, it is likely that the two are at least loosely associated (Kleineidam et al., 2007).

If an increase in the number of sensilla is indeed accompanied by an increase in ORNs this could have a number of consequences including greater sensitivity, an improved ability to discriminate between compounds or sensitivity to a greater number of compounds (Kelber et al., 2006). Previous studies have linked increased sensillum numbers in larger workers within species to increased olfactory sensitivity leading to differences in foraging and trail following efficiencies (leaf-cutting ants: Kleineidam et al., 2007; bumblebees: Spaethe et al., 2007). Studying the underlying neuroanatomy and differences in behavioural responses to odour cues may reveal further differences in *T. rugatulus* workers which may help explain differences in task allocation.

4.1.1. An undescribed type of sensillum in ants: palmate sensilla

We observed the scape of *T. rugatulus* a branched type of sensillum that has not been found in other ants (Jaisson, 1969; Dumpert, 1972; Hashimoto, 1990; Kleineidam et al., 2000; Renthal et al., 2003; Marques-Silva et al., 2006; Nakanishi et al., 2009; Mysore et al., 2010; Barsagade et al., 2013; Ramirez-Esquivel et al., 2014). This sensillum closely resembles the palmate sensilla seen in the weevil *Pissodes nitidus* (Coleoptera) (Yan et al., 2011). Yan et al. (2011) suggest that these may be olfactory sensilla as there are grooves on the surface of the sensillum and ultrathin sections indicate the presence of openings connecting the exterior to the lumen typical of olfactory sensilla. Consistent with this, the palmate sensilla of *T. rugatulus* have longitudinal grooves covering the surface (Fig. 5C, inset) but analysis of the internal anatomy will be necessary to determine if these grooves do contain openings into the lumen.

Upon further examination we observed other branched sensilla on the head, mesosoma, petiole and gaster. However, these were quite different in form to those on the scape, suggesting that they may not be homologous. While the palmate sensilla found on the scape are shaped like a scoop (Fig. 5A, C), the branched sensilla found elsewhere roughly resemble a pyramidal prism, where the three sides are strongly concave (Fig. 5D, G, H). Furthermore, while the palmate sensilla on the weevil *P. nitidus* numbered in the hundreds and covered the apical segment of the antenna, the palmate sensilla we observed on the scape were very rare (maximum of 3). Yan et al. (2011) also classified their palmate sensilla according to the number of finger-like protrusions. They describe sensilla with 1, 2, 3, and 4 digits and about 200 sensilla in each category, while the sensilla in *T. rugatulus* varied seemingly randomly in the number of digits from 3 to 10. It is not clear then whether the *P. nitidus* and *T. rugatulus* palmate sensilla are homologous but their resemblance is such that we feel it is appropriate for them to share a name. Although the branched sensilla found on the head, mesosoma, petiole and gaster look somewhat different, until further studies show whether they are functionally different or not it seems convenient to refer to them under the same name.

To the best of our knowledge this is the first time palmate sensilla have been described in Formicidae. It is possible that they

have been overlooked in other ants due to their location outside of the flagellum. Preliminary observations showed that palmate sensilla are present on the head, mesosoma, petiole, and gaster in other small ant species (*Pheidole* sp., *Paraparatrechina minitula*, *Technomyrmex* sp.), but not in all (*Meranoplus ferrugineus*) (Ramirez-Esquivel, unpublished observation). However, in none of these species were palmate sensilla found on the scape, making T. *rugatulus* an exception.

4.2. The optical system

Vision is crucial for most ants to navigate between food resources and the nest, be it in exclusively solitary foraging species or for scouts in species that recruit by laying pheromone trails. The majority of studies on visual navigation to date have focussed on ants with large eyes (e.g. *Cataglyphis bicolor*: 1300 facets (Menzi, 1987), *Camponotus consobrinus:* 798 facets (Narendra et al., 2016), *Formica integroides*: 700 facets (Bernstein and Finn, 1971), *Gigantiops destructor*: 4100 facets (Gronenberg and Hölldobler, 1999), *Melophorus bagoti*: 590 facets (Schwarz et al., 2011), *Myrmecia croslandi*: 2363 facets, *Myrmecia pyriformis*: 3593 facets (Greiner et al., 2007; Narendra et al., 2011), *Polyrhachis sokolova*: 596 facets (Narendra et al., 2013)). *Temnothorax* is one of the very few ants that we are aware of, that have been shown to navigate visually with just over 50 ommatidia in each eye. *Temnothorax albipennis*, for instance, does indeed use visual landmarks for navigation (Pratt et al., 2001). *T. rugatulus* tends to forage individually in an environment where the undergrowth is relatively sparse, with few proximate landmarks. Foraging workers therefore most likely rely on distant cues that appear above the horizon, such as tree trunks, for navigation.

We observed considerable variation in the number of facets per eye in these ants (range = 45–76), which raises the question of what impact such significant variations in the 'number of pixels' and the sensitivity between individuals within a single colony may have on task allocation (e.g. Perl and Niven, 2016). It is important to note in this context that visual navigation does not necessarily require high-resolution vision (e.g. Milford, 2013; Stürzl et al., 2015; Wystrach et al., 2016). However, differences in resolution do affect target detection (e.g. Spaethe and Chittka, 2003), which may impact worker foraging efficiency. This will be dependent on the foraging strategies employed by *Temnothorax* ants in natural conditions, which are unfortunately not well studied. Detection of small objects and detection distances will be improved in workers with greater visual resolution. Adding a word of caution in this context, we note that we had to estimate compound eye properties such as visual fields and inter-ommatidial angles from SEM preparations and light-microscopy sections, because *in-vivo* optical analysis is practically impossible in these small heavily pigmented eyes. It thus remains to be investigated how the number of ommatidia and eye curvature vary in these ants which will both determine the variations in resolution and visual fields. Studying foraging behaviours and visual tasks in a natural setting should tell us more about what is required from the compound eyes of *Temnothorax* ants.

The lens diameters of the ants do not vary with head width, but vary within each individual. Their lens diameters in the compound eyes of *T. rugatulus* (range: 14.7–19.0 μm) place them in the company of much larger day-active ants (e.g., *M. bagoti*: 19 μm (Schwarz et al., 2011); *M. croslandi*: 18 μm (Greiner et al., 2007)). However, their large rhabdom diameter and in particular the very short effective focal length in these eyes generate an optical sensitivity that is much higher (S = 4.1 μm^2 sr^{-1}) than that found in large nocturnal ants (e.g. *M. pyriformis*: S = 1–1.6 μm^2 sr^{-1}; (Greiner et al., 2007)) and nocturnal bees (e.g. *Megalopta genalis*, S = 2.7 μm^2 sr^{-1}; (Greiner et al., 2004)). This unexpectedly high sensitivity in *T. rugatulus* may be an adaptation for the dim-lit leaf litter habitat in which these ants forage. In *T. rugatulus* facet diameters did not vary with head width, but if rhabdom diameters decreased in smaller individuals, this would reduce their optical sensitivity.

Our modelling of the optical properties of *T. rugatulus* ommatidia indicates that given the assumption of uniform refractive indices, the lens and crystalline cone do not focus light on the distal tip of the rhabdom, but at a point about 10 μm down the length of the rhabdom. This severe under-focussing has not been found in other miniature compound eyes (e.g. Fischer et al., 2011; Makarova et al., 2015). However, a discussion of the functional significance of this arrangement would be premature, because we do not know whether there is a refractive index gradient in the facet lenses of *T. rugatulus* ommatidia that would increase the refractive power of the optical system, bringing the focal plane closer to the distal tip of the rhabdom.

We also found what seem to be specialised rhabdoms, which appear rectangular in cross-section (Fig. 8F). These are similar to the specialised photoreceptors found in the dorsal rim area of several ants such as *Cataglyphis fortis*, *C. consobrinus*, *M. pyriformis*, *Nothomyrmecia macrops*, and *P. sokolova* (Zeil et al., 2014; Narendra et al., 2016). In these specialised rhabdoms the microvilli of retinular cells are typically oriented at 90° relative to each other and do not twist along the length of the rhabdom, making them sensitive to the direction of polarised light. Although we were unable to confirm these properties in *T. rugatulus*, the rectangular cross sections of dorsal rhabdoms hint at the possibility that in addition to using landmark information for navigation, *Temnothorax* ants may also rely on the pattern of polarised skylight to derive compass information for path integration.

4.3. Worker size variation

Workers in our study varied in head width from 0.45 to 0.66 mm (n = 100) and had a normal frequency distribution. By comparison, Westling et al. (2014) examined worker size variation in great detail and found worker head width ranged from 0.35 to 0.70 (n = 522). Furthermore, Westling et al. (2014) also identified a small intranidal class of workers and a large extranidal class. These two subpopulations had overlapping distributions which when pooled give rise to a distribution similar to ours. However, the small intranidal workers described were much smaller than any workers we observe in our sample. The greater range in distribution and the bias towards larger workers we observe might be explained by differences in sample sizes in the two studies or it may be because the two colonies we sampled do not represent mature colonies. There may be costs associated with producing fully specialised workers before the colony has reached maturity and achieved a full complement of workers. Young and small colonies in other species have previously been shown to produce worker size distributions that differ from those of mature colonies (Wood and Tschinkel, 1981; Tschinkel, 1988, 1998).

Although the range and frequency distribution of worker head widths shown here is not fully consistent with those previously reported, this does not imply that workers in our sample were uniform. Even the limited range of body-sizes we observe seems considerable for a "monomorphic" species and is sufficient to produce variability in the sensory arrays.

5. Conclusions

We observe variability in the sensory systems of *T. rugatulus*, which is linked, to some extent, to worker head width. We suggest that these variations, both of the compound eyes and antennal

sensillum arrays, may have functional implications in terms of a worker's access to information about her social and physical environment. This may in turn play a role in worker specialisation and task allocation, although this remains to be tested using behavioural experiments, which identify not just worker size but also intra- or extranidal behavioural castes.

Acknowledgements

We are grateful to Wolfgang Rössler for hosting FRE and NEL in the University of Würzburg enabling this collaboration to take place. We thank Vivien Bauer for forwarding samples to Australia, Claudia Gehrig from the Electron Microscopy Unit in the Würzburg Biozentrum for materials for specimen preparation, and the Centre for Advanced Microscopy at the Australian National University for imaging facilities. We are grateful to Paul Cooper for discussions on the potential functions of palmate sensilla, to Eric Warrant for advice, and to Andrew May for comments on the manuscript. We acknowledge funding support for a PhD scholarship (FRE) from The Australian National University, from the Australian Research Council's (ARC) Centres of Excellence Scheme (CEO561903, JZ & AN), from the Go8 Australia Germany Joint Research Cooperation Scheme (AN & JZ), ARC DECRA and Future Fellowship Grants to AN (DE120100019, FT140100221) and from the National Science Foundation for NEL's PhD stipend (NSF DGE-1143953).

References

Barsagade, D.D., Tembhare, D.B., Kadu, S.G., 2013. Microscopic structure of antennal sensilla in the carpenter ant *Camponotus compressus* (Fabricius) (Formicidae: Hymenoptera). Asian Myrmecol. 5, 113–120.
Bernstein, S., Finn, C., 1971. Ant compound eye: size-related ommatidium differences within a single wood ant nest. Experientia 27, 708–710.
Cao, T., Dornhaus, A., 2012. Ants use pheromone markings in emigrations to move closer to food-rich areas. Insectes Sociaux 59, 87–92.
Charbonneau, D., Dornhaus, A., 2015a. When doing nothing is something. How task allocation strategies compromise between flexibility, efficiency, and inactive agents. J. Bioecon. 17, 217–242.
Charbonneau, D., Dornhaus, A., 2015b. Workers 'specialized' on inactivity: behavioral consistency of inactive workers and their role in task allocation. Behav. Ecol. Sociobiol. 69, 1459–1472.
Duchamp-Viret, P., Chaput, M., Duchamp, A., 1999. Odor response properties of rat olfactory receptor neurons. Science 284, 2171–2174.
Dumpert, K., 1972. Bau und Verteilung der Sensillen auf der Antennengeißel von *Lasius fuliginosus* (Latr.) (Hymenoptera, Formicidae). Zoomorphology 73, 95–116.
Faber, T., Joerges, J., Menzel, R., 1999. Associative learning modifies neural representations of odors in the insect brain. Nat. Neurosci. 2, 74–78.
Fischer, S., Müller, C.H., Meyer-Rochow, V.B., 2011. How small can small be: the compound eye of the parasitoid wasp *Trichogramma evanescens* (Westwood, 1833) (Hymenoptera, Hexapoda), an insect of 0.3-to 0.4-mm total body size. Vis. Neurosci. 28, 295–308.
Franks, N.R., Hooper, J.W., Dornhaus, A., Aukett, P.J., Hayward, A.L., Berghoff, S.M., 2007. Reconnaissance and latent learning in ants. Proc. R. Soc. Lond. B Biol. Sci. 274, 1505–1509.
Galizia, C.G., Menzel, R., 2000. Odour perception in honeybees: coding information in glomerular patterns. Curr. Opin. Neurobiol. 10, 504–510.
Getz, W.M., Akers, R.P., 1995. Partitioning non-linearities in the response of honey bee olfactory receptor neurons to binary odors. Biosystems 34, 27–40.
Greiner, B., Narendra, A., Reid, S.F., Dacke, M., Ribi, W.A., Zeil, J., 2007. Eye structure correlates with distinct foraging-bout timing in primitive ants. Curr. Biol. 17, R879–R880.
Greiner, B., Ribi, W.A., Warrant, E.J., 2004. Retinal and optical adaptations for nocturnal vision in the halictid bee *Megalopta genalis*. Cell Tissue Res. 316, 377–390.
Gronenberg, W., Hölldobler, B., 1999. Morphologic representation of visual and antennal information in the ant brain. J. Comp. Neurol. 412, 229–240.
Hashimoto, Y., 1990. Unique features of sensilla on the antennae of Formicidae (Hymenoptera). Appl. Entomol. Zool. 25, 491–501.
Hölldobler, B., Wilson, E.O., 1990. The Ants. The Belknap Press of Harvard University Press, Cambridge, Massachusetts.
Jaisson, P., 1969. Étude de la distribution des organes sensoriels de l'antenne et de leurs relations possibles avec le comportement chez deux fourmis myrmicines: *Myrmica laevinodis* Nyl. et *Aphaenogaster gibbosa* Latr. récoltées dans la région des Eyzies. Insectes Sociaux 16, 279–312.
Kaspari, M., Weiser, M., 1999. The size–grain hypothesis and interspecific scaling in ants. Funct. Ecol. 13, 530–538.
Kelber, C., Rössler, W., Kleineidam, C.J., 2006. Multiple olfactory receptor neurons and their axonal projections in the antennal lobe of the honeybee *Apis mellifera*. J. Comp. Neurol. 496, 395–405.
Kleineidam, C., Romani, R., Tautz, J., Isidoro, N., 2000. Ultrastructure and physiology of the CO_2 sensitive sensillum ampullaceum in the leaf-cutting ant *Atta sexdens*. Arthropod Struct. Dev. 29, 43–55.
Kleineidam, C., Rössler, W., Hölldobler, B., Roces, F., 2007. Perceptual differences in trail-following leaf-cutting ants relate to body size. J. Insect Physiol. 53, 1233–1241.
Land, M.F., 1981. Optics and vision in invertebrates. In: Autrum, H. (Ed.), Handbook of Sensory Physiology. Springer, Berlin Heidleberg New York, pp. 471–592.
Land, M.F., Nilsson, D.-E., 2012. Animal Eyes, second ed. Oxford University Press, Oxford.
Lewis, C., 1971. Superficial sense organs of the antennae of the fly, *Stomoxys calcitrans*. J. Insect Physiol. 17, 449–461.
Makarova, A., Polilov, A., Fischer, S., 2015. Comparative morphological analysis of compound eye miniaturization in minute hymenoptera. Arthropod Struct. Dev. 44, 21–32.
Maleszka, R., 2016. Epigenetic code and insect behavioural plasticity. Curr. Opin. Insect Sci. 15, 45–52.
Marques-Silva, S., Matiello-Guss, C.P., Delabie, J.H.C., Mariano, C.S.F., Zanuncio, J.C., Serrão, J.E., 2006. Sensilla and secretory glands in the antennae of a primitive ant: *Dinoponera lucida* (Formicidae: Ponerinae). Microsc. Res. Tech. 69, 885–890.
Maschwitz, U., Lenz, S., Buschinger, A., 1986. Individual specific trails in the ant *Leptothorax affinis* (Formicidae: Myrmicinae). Experientia 42, 1173–1174.
Menzi, U., 1987. Visual adaptation in nocturnal and diurnal ants. J. Comp. Physiol. A 160, 11–21.
Milford, M., 2013. Vision-based place recognition: how low can you go? Int. J. Robot. Res. 32, 766–789.
Möglich, M., Maschwitz, U., Hölldobler, B., 1974. Tandem calling: a new kind of signal in ant communication. Science 186, 1046–1047.
Mysore, K., Shyamala, B.V., Rodrigues, V., 2010. Morphological and developmental analysis of peripheral antennal chemosensory sensilla and central olfactory glomeruli in worker castes of *Camponotus compressus* (Fabricius, 1787). Arthropod Struct. Dev. 39, 310–321.
Nakanishi, A., Nishino, H., Watanabe, H., Yokohari, F., Nishikawa, M., 2009. Sex-specific antennal sensory system in the ant *Camponotus japonicus*: structure and distribution of sensilla on the flagellum. Cell Tissue Res. 338, 79–97.
Narendra, A., Alkaladi, A., Raderschall, C.A., Robson, S.K.A., Ribi, W.A., 2013. Compound eye adaptations for diurnal and nocturnal lifestyle in the intertidal ant, *Polyrhachis sokolova*. PLoS One 8, e76015.
Narendra, A., Ramirez-Esquivel, F., Ribi, W.A., 2016. Compound eye and ocellar structure for walking and flying modes of locomotion in the Australian ant, *Camponotus consobrinus*. Sci. Rep. 6, 22331.
Narendra, A., Reid, S.F., Greiner, B., Peters, R.A., Hemmi, J.M., Ribi, W.A., Zeil, J., 2011. Caste-specific visual adaptations to distinct daily activity schedules in Australian *Myrmecia* ants. Proc. R. Soc. B Biol. Sci. 278, 1141–1149.
Perl, C.D., Niven, J.E., 2016. Differential scaling within an insect compound eye. Biol. Lett. 12, 20160042.
Pix, W., Zanker, J.M., Zeil, J., 2000. The optomotor response and spatial resolution of the visual system in male *Xenos vesparum* (Strepsiptera). J. Exp. Biol. 203, 3397–3409.
Pratt, S.C., Brooks, S.E., Franks, N.R., 2001. The use of edges in visual navigation by the ant *Leptothorax albipennis*. Ethology 107, 1125–1136.
Ramirez-Esquivel, F., Zeil, J., Narendra, A., 2014. The antennal sensory array of the nocturnal bull ant *Myrmecia pyriformis*. Arthropod Struct. Dev. 43, 543–558.
Renthal, R., Velasquez, D., Olmos, D., Hampton, J., Wergin, W.P., 2003. Structure and distribution of antennal sensilla of the red imported fire ant. Micron 34, 405–413.
Sachse, S., Rappert, A., Galizia, C.G., 1999. The spatial representation of chemical structures in the antennal lobe of honeybees: steps towards the olfactory code. Eur. J. Neurosci. 11, 3970–3982.
Sasaki, T., Hölldobler, B., Millar, J.G., Pratt, S.C., 2014. A context-dependent alarm signal in the ant *Temnothorax rugatulus*. J. Exp. Biol. 217, 3229–3236.
Schneider, D., 1964. Insect antennae. Annu. Rev. Entomol. 9, 103–122.
Schwarz, S., Narendra, A., Zeil, J., 2011. The properties of the visual system in the Australian desert ant *Melophorus bagoti*. Arthropod Struct. Dev. 40, 128–134.
Spaethe, J., Brockmann, A., Halbig, C., Tautz, J., 2007. Size determines antennal sensitivity and behavioral threshold to odors in bumblebee workers. Naturwissenschaften 94, 733–739.
Spaethe, J., Chittka, L., 2003. Interindividual variation of eye optics and single object resolution in bumblebees. J. Exp. Biol. 206, 3447–3453.
Stavenga, D., 2003. Angular and spectral sensitivity of fly photoreceptors. II. Dependence on facet lens F-number and rhabdomere type in *Drosophila*. J. Comp. Physiol. A 189, 189–202.
Steinbrecht, R.A., 1973. Der Feinbau olfaktorischer Sensillen des Seidenspinners (Insecta, Lepidoptera). Z. für Zellforsch. Mikrosk. Anat. 139, 533–565.
Stroeymeyt, N., Franks, N.R., Giurfa, M., 2011. Knowledgeable individuals lead collective decisions in ants. J. Exp. Biol. 214, 3046–3054.
Stroeymeyt, N., Jordan, C., Mayer, G., Hovsepian, S., Giurfa, M., Franks, N., 2014. Seasonality in communication and collective decision-making in ants. Proc. R. Soc. Lond. B Biol. Sci. 281, 20133108.

Stürzl, W., Grixa, I., Mair, E., Narendra, A., Zeil, J., 2015. Three-dimensional models of natural environments and the mapping of navigational information. J. Comp. Physiol. A 201, 563–584.
Tschinkel, W., 1998. Sociometry and sociogenesis of colonies of the harvester ant, *Pogonomyrmex badius*: worker characteristics in relation to colony size and season. Insectes Sociaux 45, 385–410.
Tschinkel, W.R., 1988. Colony growth and the ontogeny of worker polymorphism in the fire ant, *Solenopsis invicta*. Behav. Ecol. Sociobiol. 22, 103–115.
Tschinkel, W.R., Mikheyev, A.S., Storz, S.R., 2003. Allometry of workers of the fire ant, *Solenopsis invicta*. J. Insect Sci. 3, 2.
van der Woude, E., Smid, H.M., 2015. How to escape from Haller's rule: olfactory system complexity in small and large *Trichogramma evanescens* parasitic wasps. J. Comp. Neurol. 524, 1876–1891.
Warrant, E., Dacke, M., 2011. Vision and visual navigation in nocturnal insects. Annu. Rev. Entomol. 56, 239–254.
Warrant, E.J., Nilsson, D.-E., 1998. Absorption of white light in photoreceptors. Vis. Res. 38, 195–207.
Westling, J., Harrington, K., Bengston, S., Dornhaus, A., 2014. Morphological differences between extranidal and intranidal workers in the ant *Temnothorax rugatulus*, but no effect of body size on foraging distance. Insectes Sociaux 61, 367–369.
Wood, L.A., Tschinkel, W.R., 1981. Quantification and modification of worker size variation in the fire ant *Solenopsis invicta*. Insectes Sociaux 28, 117–128.
Wystrach, A., Dewar, A., Philippides, A., Graham, P., 2016. How do field of view and resolution affect the information content of panoramic scenes for visual navigation? A computational investigation. J. Comp. Physiol. A 202, 87–95.
Yan, S.C., Meng, Z.J., Peng, L., Liu, D., 2011. Antennal sensilla of the pine weevil *Pissodes nitidus* Roel. (Coleoptera: Curculionidae). Microsc. Res. Tech. 74, 389–396.
Zeil, J., Ribi, W.A., Narendra, A., 2014. Polarisation vision in ants, bees and wasps. In: Horváth, G. (Ed.), Polarized Light and Polarization Vision in Animal Sciences. Springer, pp. 41–60.